Immunity 25, 429–440, September 2006 ©2006 Elsevier Inc. DOI 10.1016/j.immuni.2006.07.014

Toll-like Receptor 7-Dependent Loss of B Cell Tolerance in Pathogenic Autoantibody Knockin Mice

Robert Berland,[1] Luis Fernandez,[1,2,6] Elina Kari,[1,7] Jin-Hwan Han,[1,2] Ina Lomakin,[3] Shizuo Akira,[4] Henry H. Wortis,[1,2] John F. Kearney,[5] Angelo A. Ucci,[3] and Thereza Imanishi-Kari[1,2,*]

[1] Department of Pathology
[2] Program in Immunology of Sackler School of Graduate Biomedical Sciences
Tufts University School of Medicine
Boston, Massachusetts 02111
[3] Department of Pathology
Tufts-NEMCH
750 Washington Street
Boston, Massachusetts 02111
[4] Department of Host Defense
Research Institute for Microbial Diseases
Osaka University
Osaka 565-0871
Japan
[5] Department of Microbiology
University of Alabama at Birmingham
Birmingham, Alabama 35294

Summary

Systemic lupus erythematosus (SLE) is characterized by the production of autoantibodies that are frequently directed against nucleic acid-associated antigens. To better understand how B cells reactive with such antigens are regulated, we generated a model system in which heavy and light chain genes encoding 564 immunoglobulin have been targeted to the heavy and light chain loci of the nonautoimmune C57BL/6 mouse strain. This antibody recognizes RNA, single-stranded DNA, and nucleosomes. We show that B cells expressing this immunoglobulin were activated, producing class-switched autoantibody in vivo despite the apparently normal induction of anergy. This autoantibody production was largely dependent on Toll-like receptor 7 (TLR7). We further show that production of these autoantibodies was sufficient to cause kidney pathology in these mice. These results demonstrate that the particular threat of nucleic acid-containing autoantigens lies in their ability to bind both antigen receptor and TLR7.

Introduction

Toll-like receptors (TLRs) are pattern-recognition receptors that bind to molecular structures associated with pathogens and alert the immune system to the presence of infection (Takeda et al., 2003). The TLR family has 11 recognized members. Most TLR ligands, such as lipopolysaccharide (LPS, recognized by TLR4), flagellin (recognized by TLR5), and bacterial lipoproteins and lipoteichoic acids (recognized by TLR2), are unique to pathogens. In contrast, TLR7 and TLR9 recognize single-stranded RNA (ssRNA) and double-stranded DNA (dsDNA), respectively, which are present in the host as well (Takeda et al., 2003). Activation of these receptors by host nucleic acid is avoided, in large part, by their intracellular localization (Barton et al., 2006; Heil et al., 2004). However, recent in vitro experiments have demonstrated that if host DNA or RNA is delivered to the appropriate compartment by receptor-mediated endocytosis, activation results, as measured by either cellular proliferation in the case of B cells (Lau et al., 2005; Leadbetter et al., 2002; Viglianti et al., 2003) or cytokine production in the case of dendritic cells (DC) or plasmacytoid dendritic cells (pDC) (Boule et al., 2004; Vollmer et al., 2005). This provides a potential mechanism for the activation of B cells expressing a B cell receptor (BCR) reactive with nucleic acid-containing antigens such as nucleosomes or Smith antigen ribonucleoprotein (SmRNP). These "dual specificity" antigens could potentially activate autoreactive B cells as a result of their ability to ligate both the BCR and, after endocytosis, either TLR9 or TLR7. B cells reactive with such antigens are commonly generated as a result of random recombination of V(D)J gene segments during B cell development (Wardemann et al., 2003) and may also arise in the periphery as a result of hypermutation in germinal centers. A variety of B cell tolerance mechanisms are believed to prevent these cells from becoming activated under normal circumstances (Goodnow et al., 2005).

In order to better understand how B cells reactive with nucleic acid-containing antigens are regulated in nonautoimmune-prone mice, we have generated a new site-directed immunoglobulin transgenic mouse line, 564Igi. The V(D)J used in 564 Igi mice was cloned from a hybridoma derived from an autoimmune SWRxNZB (SNF1) mouse (Gavalchin et al., 1987). It produces a pathogenic (Vlahakos et al., 1992) polyreactive antibody that reacts with ssDNA (Gavalchin et al., 1987), ssRNA (Gavalchin et al., 1987), and nucleosomes (Mohan et al., 1993). Several other Ig-transgenic mouse lines have been generated with BCRs specific for nucleic acid or other specificities commonly recognized by autoantibodies in patients with SLE (reviewed in Fields and Erikson, 2003). These include anti-dsDNA, anti-ssDNA, anti-Sm, and Rheumatoid Factor (RF). Depending on the model system, the general result is that, on nonautoimmune backgrounds, the production of immunoglobulin G (IgG) autoantibodies is prevented by either Ig receptor editing, deletion, induction of B cell anergy, or, in the case of anti-Sm, differentiation to the B-1a population (Fields and Erikson, 2003). As in these other systems, in the present study 564-expressing B cells underwent receptor editing, resulting in a large fraction of 564-negative cells. Those cells that retained the 564Igi idiotype were anergic based on their surface phenotype, exclusion from the marginal zone (MZ), and lack of response to BCR crosslinking or LPS in vitro.

*Correspondence: thereza.imanishi-kari@tufts.edu
[6] Present address: TBRC, Massachusetts General Hospital, Boston, Massachusetts 02114.
[7] Present address: Emory University School of Medicine, Atlanta, Georgia 30322.

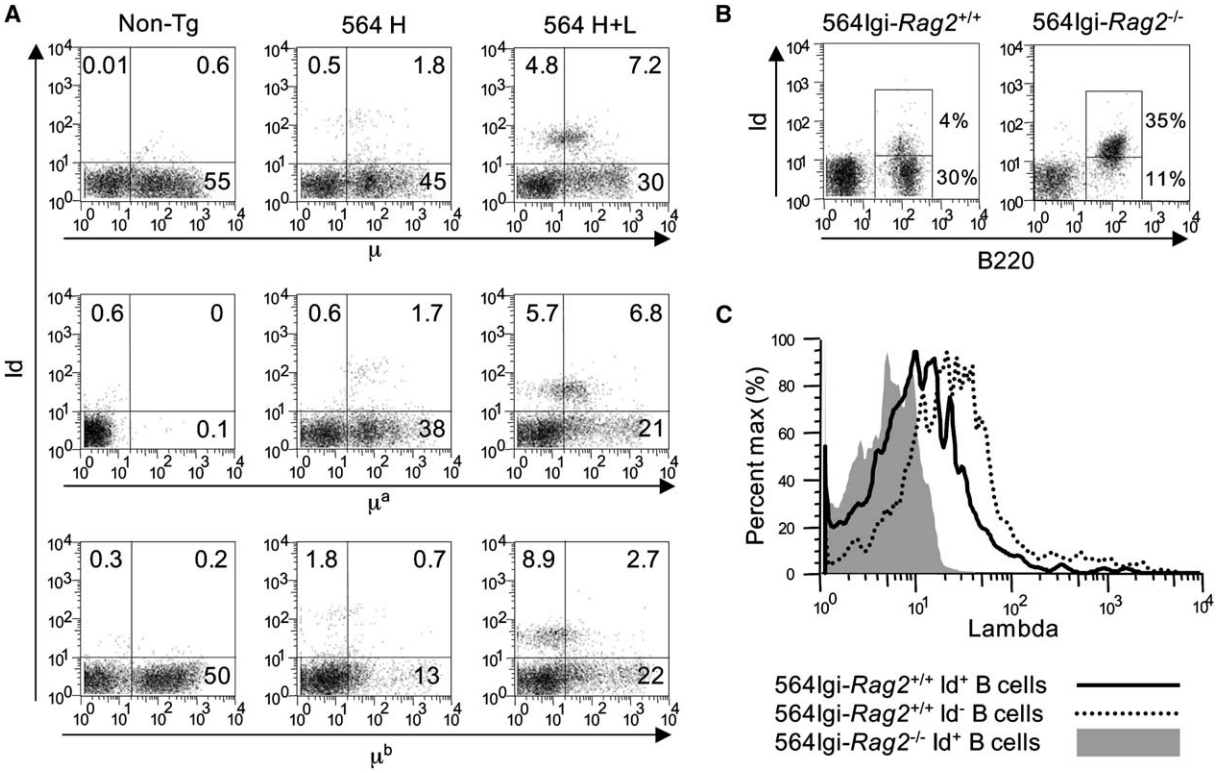

Figure 1. Receptor Editing in 564Igi Mice

(A) Specificity of the B6-256 (anti-Id) monoclonal antibody. Splenocytes from a nontransgenic C57BL/6 mouse, a mouse heterozygous for the 564 heavy chain (564H), and a mouse expressing both heavy and light chains of 564 (564HL) were stained with B6-256 and antibodies against μ, μ^a, or μ^b and analyzed by flow cytometry. Viable (PI-excluding) lymphocytes are shown. The percentage of cells in each quadrant is indicated.

(B) Effect of RAG2 deficiency on the frequency of Id^+ splenocytes. Splenocytes from mice of the indicated genotypes were stained as indicated and analyzed by flow cytometery. Viable lymphocytes are shown. Percentages of cells in each gate are shown.

(C) Endogenous λ light chain gene expression in 564Igi mice. Splenocytes from 564Igi-*Rag2*$^{-/-}$ and 564Igi-*Rag2*$^{+/+}$ mice were stained with B6-256 anti-Id, anti-CD45 (B220), and anti-λ light chain and analyzed by flow cytometry. Histograms are gated on viable $B220^+$ lymphocytes that were either Id^+ or Id^- as indicated. All results are representative of at least three independent experiments.

Strikingly, despite this induction of anergy, we found considerable amounts of 564 idiotype-positive T_H1-skewed IgG antibody in the serum of 564Igi mice. Production of these antibodies was largely dependent on TLR7. This represents the first in vivo evidence that TLR7 can drive the production of nuclear antibodies. We were also able to detect evidence of kidney pathology in mice producing these autoantibodies. This pathology was similar to what is seen in SLE-associated kidney disease in humans.

Results

Construction of 564Igi Mice

Mice carrying a targeted insertion of the 564 V(D)J have been described elsewhere (Fernandez, 2001). The generation of mice carrying a targeted insertion of the 564 light chain is shown in Figure S1 in the Supplemental Data available online. Mice carrying either the targeted heavy or light chain locus were backcrossed to C57BL/6 mice by means of a speed congenic procedure (Wakeland et al., 1997) for more than 10 generations as described and then intercrossed to generate mice with targeted insertions at both loci.

Receptor Editing and Anergy in 564Igi Mice

We expected that expression of 564 heavy and light chains would result in B cell tolerance on the nonautoimmune C57BL/6 background as a result of receptor editing (Casellas et al., 2001; Chen et al., 1997) and/or clonal anergy (Chen et al., 1997; Goodnow et al., 2005). To determine whether receptor editing occurs in the 564Igi system, we stained splenocytes with an anti-idiotype antibody. This antibody stained B cells only in mice containing targeted insertions of both the heavy and light chain genes of the 564 antibody (Figure 1A). Furthermore, only B cells expressing the transgene-derived heavy chain (*a* allotype) were stained (Figure 1A). Consistent with receptor editing, a substantial fraction of B cells in heavy plus light chain insertion mice expressed endogenous (*b* allotype) heavy chains and only a minority of cells expressing the a allotype 564 heavy chain were idiotype positive (Id^+) (Figure 1A). To confirm that the absence of Id^+ cells was due to secondary rearrangements of endogenous Ig genes, we examined 564Igi mice on a RAG2-deficient (*Rag2*$^{-/-}$) background. On this background, essentially all B cells were 564 Id^+ (Figure 1B). Consistent with extensive editing in RAG2-sufficient 564Igi mice, lambda light chain was expressed on many Id^- B cells

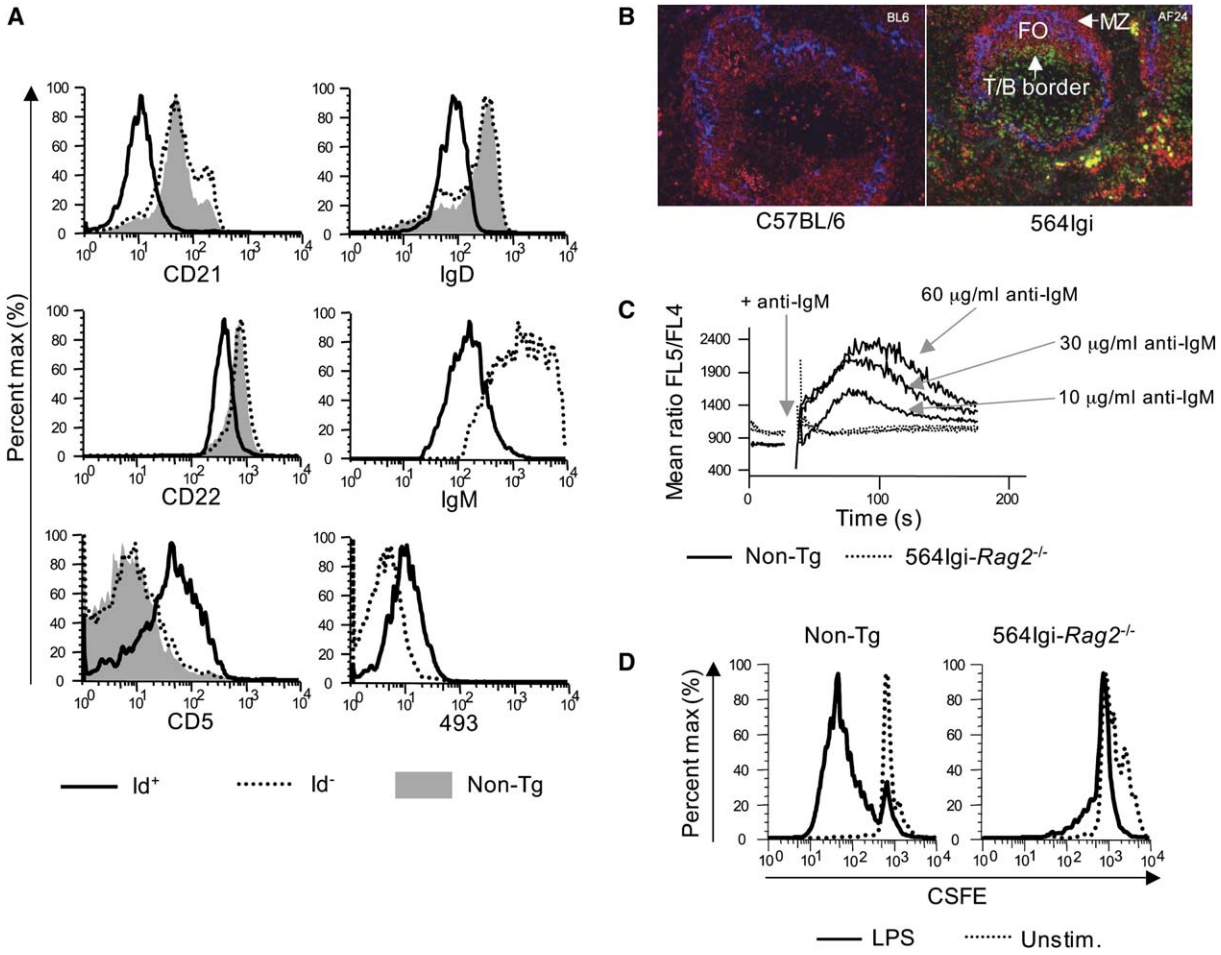

Figure 2. B Cells in 564Igi Mice Were Anergic

(A) Flow cytometry analysis of expression of the indicated surface markers on Id^+ (solid lines) or Id^- (dotted lines) splenic B cells from a 564Igi mouse and, where indicated, on splenic B cells from a nontransgenic C57BL/6 mouse (shaded histograms).

(B) 564Igi Id^+ cells were excluded from splenic B cell follicles and MZs. Frozen spleen sections from a nontransgenic C57BL/6 and a 564Igi mouse were stained with anti-IgM (red), B6-526 anti-id (green), and MOMA (blue).

(C) 564Igi B cells failed to flux calcium in response to BCR crosslinking. Indo-1-loaded RBC-depleted splenocytes from a nontransgenic C57BL/6 mouse (solid lines) and a 564Igi-*Rag2*$^{-/-}$ mouse (dotted lines) were stained with anti-CD45 (B220) and stimulated with 10, 30, or 60 μg/ml of anti-IgM. Calcium flux was monitored on $B220^+$ cells by flow cytometry. Although anti-IgM concentration is not indicated for the 564Igi samples, three essentially identical tracings, corresponding to the three different anti-IgM concentrations, are shown.

(D) 564Igi B cells respond poorly to LPS. RBC-depleted splenocytes from a nontransgenic C567BL/6 mouse and a 564Igi-*Rag2*$^{-/-}$ mouse were loaded with CFSE and cultured for 3.5 days with or without LPS. Cells were stained with B220 and CFSE fluorescence of viable (PI-excluding) $B220^+$ cells determined by flow cytometry. All results are representative of at least three independent experiments.

(Figure 1C). There was also a fraction of Id^+ cells expressing lambda light chain (Figure 1C).

In other systems, peripheral autoreactive B cells that fail to edit become anergic (Goodnow et al., 2005). We therefore examined Id^+ B cells for features of anergy as shown in Figure 2A. Id^- B cells (dotted histograms) stained similarly to C57BL/6 B cells (shaded histograms). Id^+ B cells had reduced surface expression of CD21/CD35, CD22, and IgD along with increased expression of CD93 (493, Figure 2A), consistent with developmental arrest at an immature stage (Fields and Erikson, 2003; Phan et al., 2003). 564 Id^+ cells also had the reduced expression of IgM and increased expression of CD5 that are additional features of anergic B cells (Fields and Erikson, 2003; Hippen et al., 2000; Phan et al., 2003; Yachimovich et al., 2002).

Anergic B cells are excluded from B cell follicles and the MZ in the spleen (Cyster et al., 1994; Fields and Erikson, 2003). Figure 2B shows a spleen section from a 564Igi mouse stained with anti-Id (green), anti-IgM (red), and MOMA (blue). Consistent with their anergic surface phenotype, 564 Id^+ cells were located predominantly at the T-B border and were mostly absent from the follicle and MZ.

In some cases, autoreactive B cells become sequestered in the peritoneum as B-1 cells (Murakami et al., 1992; Qian et al., 2001). We found no 564 Id^+ B-1 cells in the peritonea of 564Igi mice (data not shown).

We next examined the ability of 564 Id^+ B cells to flux calcium in response to BCR crosslinking in vitro (Figure 2C). In this experiment, we used splenocytes from a 564Igi mouse that was RAG2 deficient, because

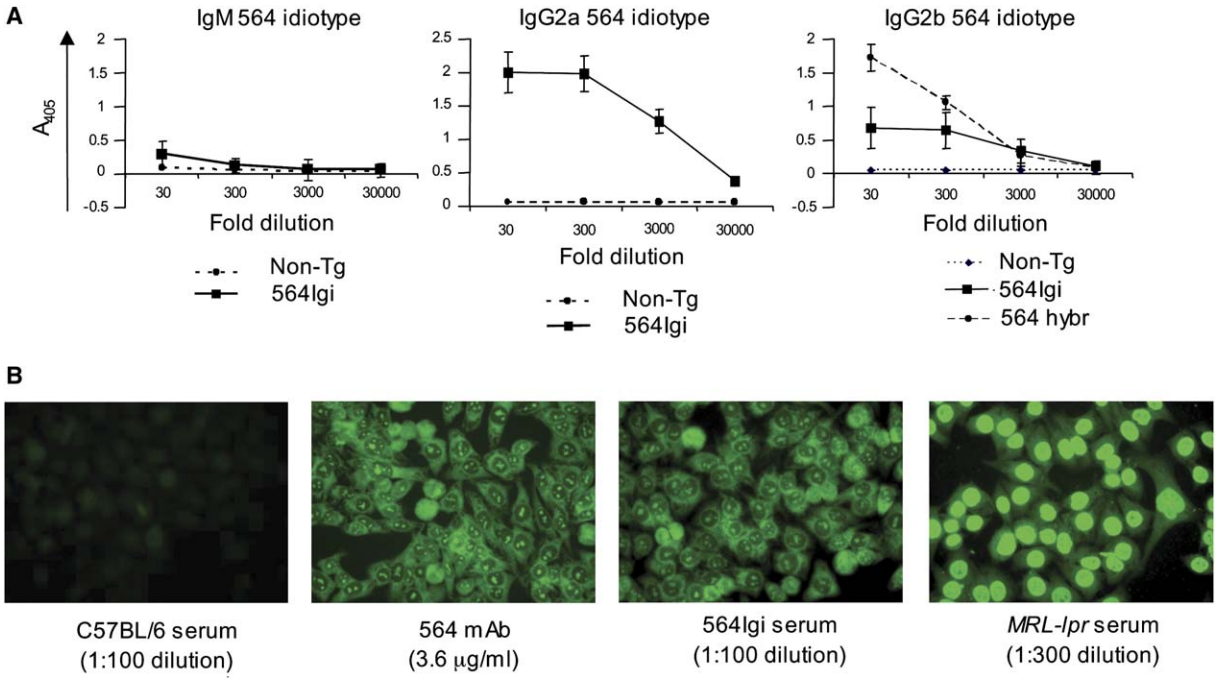

Figure 3. 564 Antibody in the Serum of 564Igi Mice

(A) ELISA assay of serum 564 Id^+ antibody. Serum from either a nontransgenic C57BL/6 (IgH^b) or a 564Igi mouse was diluted as indicated and Id^+ antibodies of the indicated isotypes measured by ELISA. Sera of 3–5 mice of each genotype were tested. Mean OD ± SD is presented. There was no signal above background when our anti-IgG2a reagent was used to detect binding of BALB/c (IgH^a) in the ELISA (data not shown). The dilutions of the 564 hybridoma supernatant correspond to 12, 1.2, 0.12, and 0.012 μg/ml.

(B) Serum antibody in 564Igi mice was autoreactive. Sera from mice of the indicated genotypes were diluted as indicated and used to stain fixed HEp-2 cells. For comparison, HEp-2 cells were stained with 564 hybridoma supernatant. Results are representative of at least three independent experiments.

all B cells from this mouse were 564 Id^+. As a control we used splenocytes from a nontransgenic C57BL/6 mouse. Cells were loaded with the calcium-sensitive dye Indo-1, stained with anti-B220, and activated with different concentrations of $F(ab')_2$ anti-IgM (anti-IgM). Calcium fluxes were measured in gated $B220^+$ cells by flow cytometry. 564Igi B cells did not flux calcium at any of the doses of anti-IgM used (Figure 2C). As in other systems (Gauld et al., 2005; Healy et al., 1997), 564Igi B cells exhibited elevated basal intracellular calcium. This suggests that 564Igi B cells were continuously exposed to antigen in vivo (Gauld et al., 2005).

Anergic B cells in some transgenic models are refractory to activation by bacterial LPS (Fields and Erikson, 2003). To see whether 564Igi B cells could be stimulated by this mitogen, splenocytes from a nontransgenic C57BL/6 or a RAG2-deficient 564 Igi mouse were loaded with carboxyfluorescein diacetate succinimidyl ester (CSFE) and cultured for 3.5 days with or without LPS. Figure 2D shows that 564Igi B cells responded very poorly to LPS.

Taken together, these data show that 564Igi B cells underwent receptor editing or became anergic (as measured by multiple criteria), suggesting that tolerance induction is normal in 564Igi mice.

Serum 564 Antibody in 564Igi Mice

We next measured amounts of serum Id^+ antibody in 564Igi mice by using an enzyme-linked immunosorbant assay (ELISA) (Figure 3A). Unexpectedly, we found high amounts of IgG2a and IgG2b Id^+ antibody. Id^+ IgM was also detected in low amounts.

To confirm that the Id^+ antibody in the serum retained the specificity of the original 564 antibody, we performed immunofluorescent staining of fixed human HEp-2 cells by using anti-mouse IgG as the secondary reagent (Figure 3B). HEp-2 cell staining was minimal with control serum from a C57BL/6 nontransgenic mouse (Figure 3B, left). Antibody purified from the 564 hybridoma stained nucleoli and the cytoplasm (Figure 3B, second panel). The same staining pattern was seen with serum from a 564Igi mouse (Figure 3B, third panel). This staining pattern differs from that seen with sera from an autoimmune MRL-*lpr* mouse, which displays uniform nuclear binding (Figure 3B, right).

These results indicate that despite the apparently normal induction of B cell anergy, class-switched autoantibodies were produced in 564Igi mice.

Kidney Pathology in 564Igi Mice

To determine whether the presence of 564 Id^+ antibodies in the sera of 564Igi mice was sufficient to lead to kidney pathology, we stained frozen sections of kidneys from a 1-year-old nontransgenic C57BL/6 mouse and from three 13-month-old 564Igi mice with fluorescently labeled anti-564 Id (Figure 4, left) or anti-mouse IgG2a (Figure 4, middle). The C57BL/6 kidney sections failed to stain with either antibody (Figure 4). In contrast,

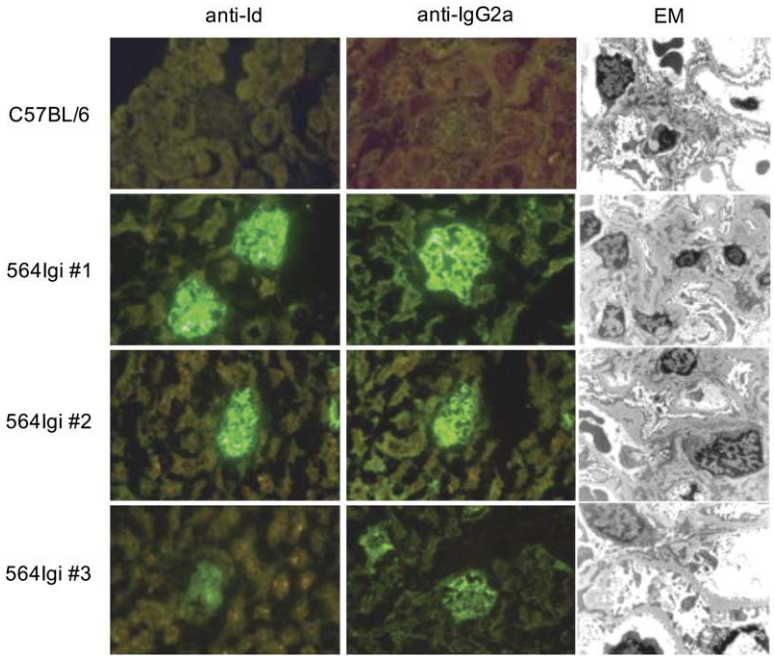

Figure 4. Kidney Pathology in 564Igi Mice

Deposition of 564 Id^+ in kidneys and kidney pathology in 564Igi mice (left and middle). Immunofluorescent staining of frozen kidney sections stained with either anti-564 Id (left) or anti-mouse IgG2a (middle). 564Igi #1, 2, and 3 are three different mice. Magnification is 465×. (Right) Electron micrographs of kidney sections from the indicated mice. Magnifications are 3307× for C57BL/6 and 564Igi #1 and 6765× for 564Igi #2 and #3.

kidney sections from all three 564Igi mice stained with both antibodies. This indicated that IgG2a 564 Id^+ antibodies were deposited in the kidneys of 564Igi mice.

To more definitively document the presence of kidney pathology, kidney sections were examined by electron microscopy (EM) (Figure 4, right, and Figure S2A). By EM, kidneys from 564Igi mice #1 and #2 showed changes consistent with those seen in mesangioproliferative glomerulonephropathies in human patients, which are associated with class 2 lupus nephritis. EM examination of the kidney from mouse #3 (Figure 4) revealed less extensive pathology, consistent with the changes seen in focal and segmental mesangioproliferative glomerulonephropathies in human patients. The C57BL/6 mouse had normal kidney architecture by EM (Figure 4). Light microscopy was consistent with the EM results (Figure S2B). A more detailed pathology report is provided in Supplemental Results as is larger version of the electron micrograph of mouse #1 shown in Figure 4 (Figure S2A).

These results indicate that the production of 564 antibody, in the absence of any other genetic predisposition to SLE, was sufficient to result in kidney pathology in 564Igi mice.

Serum 564 Antibody in 564Igi Mice on a RAG2-Deficient Background

The presence of 564 Id^+ antibody in the serum could have been a consequence of allelic inclusion, whereby a cell expressing 564 heavy and light chains rearranged an endogenous immunoglobulin heavy or light chain, resulting in the expression of two different immunoglobulin molecules. This might lower the surface density of 564 antibody sufficiently to allow escape from anergy or deletion (Liu et al., 2005). To test this possibility, we measured total serum antibodies in 564Igi-*Rag2*$^{-/-}$ mice where allelic inclusion was not possible. In these mice, all antibody produced will be 564 Id^+. Lack of RAG2 had no effect on the number of B cells in 564Igi mice (data not shown), consistent with results in a different anti-ssDNA heavy and light chain knockin mouse (Xu et al., 1998). In the serum of 564Igi-*Rag2*$^{-/-}$ mice, there were considerable titers of total IgM, IgG2a, IgG2b, IgG3, and IgA (Figure 5A). Strikingly, there was no detectable antibody of the T_H2-associated IgG1 or IgE isotypes. As a negative control, we included serum from an activation-induced cytidine deaminase (AID)-deficient (*Aicda*$^{-/-}$) mouse that was incapable of class switching. In an independent experiment to determine the effect of RAG2 deficiency specifically on the amounts of Id^+ antibody, we measured Id^+ antibodies in the sera of 564Igi-*Rag2*$^{-/-}$ and 564Igi-*Rag2*$^{+/-}$ mice (Figure S3A). Id^+ IgM, IgG3, and IgG2b were unaffected by the absence of RAG2, while Id^+ IgG2a and IgA were present at 25% to 50% of the amounts detected in 564Igi-*Rag2*$^{+/-}$ mice. Similarly, in 564Igi-*Rag2*$^{-/-}$ mice, the amounts of IgG2a cytoplasmic and nucleolar antibodies were 25% to 50% of the amounts in 564Igi-*Rag2*$^{+/-}$ mice as measured by binding to HEp-2 cells (Figure S3B).

564Igi B cells on the RAG2-deficient background retained the surface phenotype of anergic B cells with the exception of altered CD22 expression (Figure 5B) and, as shown above, were refractory to activation by anti-IgM or LPS (Figures 3C and 3D, respectively).

Thus, allelic inclusion was not responsible for the production of autoantibodies in 564Igi mice.

564Igi B Cells Were Hyperresponsive to Activation by CpG

The serum antibodies produced in 564Igi-*Rag2*$^{-/-}$ mice were skewed toward T_H1-associated isotypes and had no detectable IgG1 or IgE. These are the isotypes induced by CpG treatment of B cells in vitro (Lin et al., 2004; Liu et al., 2003). Therefore, we asked whether the anergic B cells from 564Igi-*Rag2*$^{-/-}$ mice were able to respond to CpG. Figure 6A shows the proliferative responses of 564Igi B cells and nontransgenic C57BL/6 B cells to 10 nM and 50 nM CpG oligodeoxonucleotide

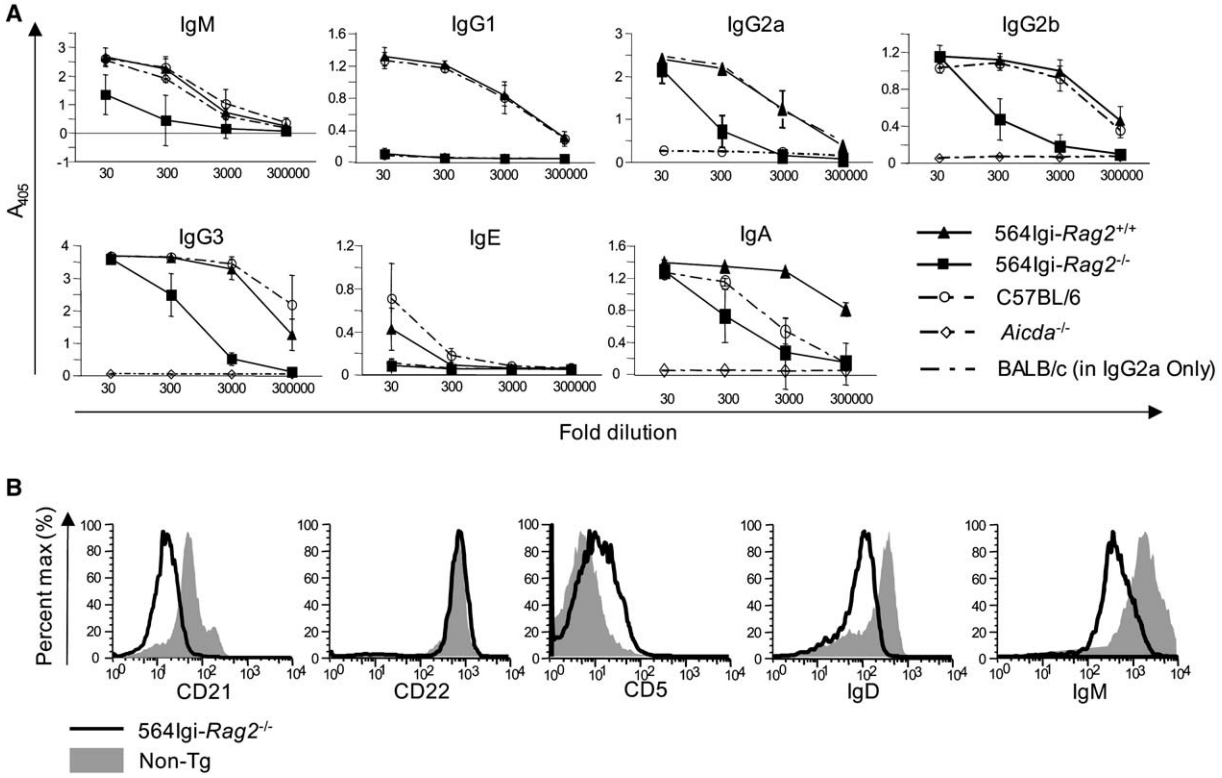

Figure 5. Isotype Skewing of Antibody Production in 564Igi-*Rag2*$^{-/-}$ Mice

(A) Amounts of total antibody of the indicated isotypes in the sera of 564Igi-*Rag2*$^{-/-}$; 564Igi-*Rag2*$^{+/+}$; nontransgenic C57BL/6, and *Aicda*$^{-/-}$ mice determined by ELISA. For IgG2a we also tested serum from an *IgH*^{a} allotype BALB/c mouse as a positive control. Values are averages ± SD for 3 C57BL/6; 3 *Aicda*$^{-/-}$; 5 564Igi-*Rag2*$^{+/+}$; and 12 564Igi-*Rag2*$^{-/-}$ mice except in the experiment to measure IgA; 5 C57BL/6, 5 *Aicda*$^{-/-}$, 2 564Igi-*Rag2*$^{+/+}$; and 7 564Igi-*Rag2*$^{-/-}$ mice were used. The experiment shown is representative of at least three independent experiments.

(B) 564Igi-*Rag2*$^{-/-}$ mice have an anergic surface phenotype. Splenocytes were isolated from a 564Igi-*Rag2*$^{-/-}$ mouse (solid lines) and a nontransgenic C57BL/6 mouse (shaded histograms), stained with the indicated antibodies, and analyzed by flow cytometry. Results are representative of at least two independent experiments.

(ODN). Substantial proliferation of 564Igi B cells occurred in response to 10 nM CpG, whereas nontransgenic B cells responded poorly to this concentration of CpG. Both 564Igi and nontransgenic B cells proliferated well in response to 50 nM CpG. A control GpC ODN failed to stimulate B cells of either genotype (Figure 6A).

The enhanced response of 564Igi B cells to CpG might have been due to BCR-mediated endocytosis of the CpG by the 564 BCR. This would be in addition to the presumed Ig receptor-independent uptake of CpG ODN, which is characteristic of non-DNA-reactive B cells. To determine whether 564 antibody binds to the CpG ODN used in the proliferation assay, we stained 564 Id^{+}-expressing B cells with fluorescently labeled CpG ODN and measured binding by flow cytometry. Figure 6B shows that CpG ODN stains 564Igi Id^{+} B cells to a greater extent than Id^{-} B cells or nontransgenic B cells.

Thus, despite their anergic phenotype, 564 Id^{+} B cells could be activated in vitro through TLR9.

564Igi B Cells Respond Synergistically to the TLR7 Agonist Loxoribine and BCR Ligation

In addition to its ability to bind to nucleosomes (Mohan et al., 1993), the 564 antibody binds to ssRNA (Gavalchin et al., 1987), and based on the predominantly cytoplasmic staining pattern apparent in Figure 4B, RNA (or RNA-associated proteins) is likely to be the physiological ligand. Thus, 564Igi B cells might become activated in vivo through TLR7. We therefore tested the ability of 564Igi B cells to be activated in vitro by the TLR7 agonist loxoribine (Akira and Hemmi, 2003; Heil et al., 2003). Splenocytes from TLR7 wild-type background 564Igi mice or TLR7-deficient 564Igi littermates were loaded with CFSE and stimulated for 3 days in vitro with loxoribine alone, a suboptimal concentration anti-IgM alone, or the combination of loxoribine and anti-IgM. Very few live (trypan blue excluding) cells were recovered from cultures of TLR7 wild-type cells cultured either without stimulation or with 2 μg/ml anti-IgM (Figure 6C). Loxoribine treatment rescued some cells, and there was a synergistic effect of the combination of loxoribine and anti-IgM on cell survival (Figure 6C). Few live cells were recovered from cultures of TLR7-deficient cells under any of the conditions (Figure 6C, open histograms). The extent of B cell proliferation in the loxoribine-treated and loxoribine plus anti-IgM-treated cultures was determined by FACS analysis of CFSE staining of viable (PI excluding) Id^{+}B220^{+} or Id^{-}B220^{+} cells (Figure 6D). Id^{-} B cells proliferated more in response to loxoribine alone than did Id^{+} cells (Figure 6D, solid line). There was a striking increase in proliferation of both Id^{-} and Id^{+} cells when cells were treated with the combination of

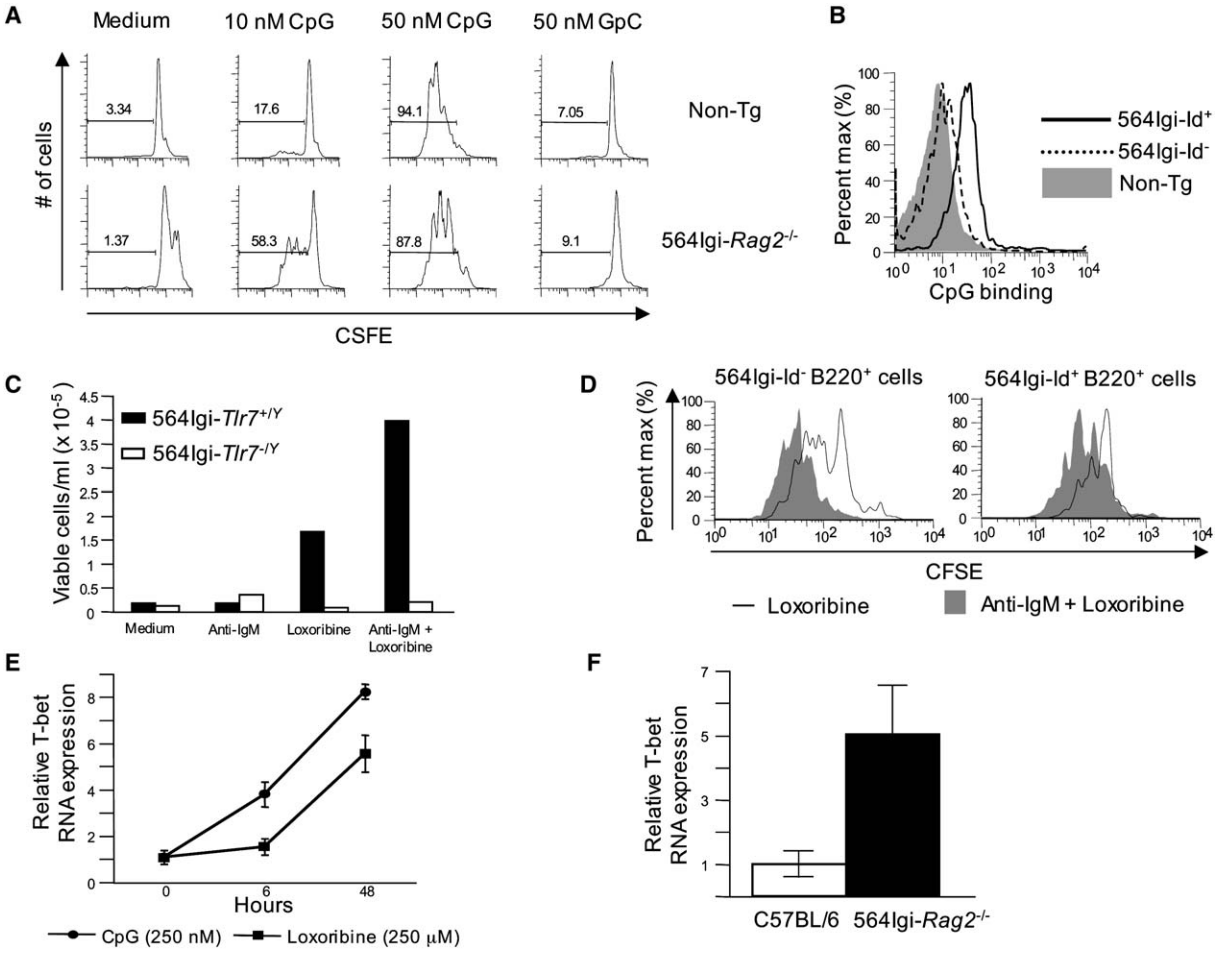

Figure 6. In Vitro Activation of 564Igi B Cells by TLR9 and TLR7 Agonists

(A) Proliferation of 564Igi-*Rag2*$^{-/-}$ B cells in response to CpG ODN. RBC-depleted splenocytes were loaded with CFSE and cultured for 3.5 days in medium alone or with the indicated concentration of CpG ODN or control GpC ODN. Cells were stained with anti-CD45 (B220) and CFSE fluorescence in viable B220$^+$ cells determined by flow cytometry. Results are representative of three experiments.

(B) Binding of CpG ODN to 564Igi-expressing B cells. RBC-depleted splenocytes from a C57BL/6 mouse (shaded histogram) and a 564Igi mouse (unfilled histograms) were stained with 1 μM fluorescein- conjugated ODN 1668, anti-B220, and anti-564Igi-Id. Viable (PI-excluding) lymphocytes are shown. For the C57BL/6 cells, CpG ODN binding on gated B220$^+$ cells is shown. For the 564Igi cells, CpG binding is shown for gated B220$^+$ 564Igi-Id$^-$ cells (dotted line) or B220$^+$ 564Igi-Id$^+$ cells (solid line).

(C) Enhanced cell survival in vitro by treatment of splenocyte cultures with loxoribine and anti-IgM. Splenocytes from a 564Igi-*Tlr7*$^{-/Y}$ mouse and a 564Igi-*Tlr7*$^{+/Y}$ littermate were depleted of red blood cells and loaded with CFSE. Cells were incubated for 3.5 days in medium alone, or with 2 μg/ml anti-IgM, 250 μM loxoribine, or both 2 μg/ml anti-IgM and 250 mM loxoribine. The concentration of live cells in each culture was determined by counting trypan blue-excluding cells in a hemocytometer. Solid bars, *Tlr7*$^{+/Y}$ splenocytes; open bars, *Tlr7*$^{-/Y}$ splenocytes.

(D) B cell proliferation in response to loxoribine or loxoribine plus anti-IgM. Proliferation of cells in the cultures described in (C) was determined by flow cytometry. Viable (PI-excluding) Id$^-$B220$^+$ or Id$^+$B220$^+$ lymphocytes are shown. The result is representative of three experiments.

(E) Induction of T-bet RNA in B cells by loxoribine and CpG ODN. Purified splenic B cells from a C57BL/6 mouse were treated with 250 μM loxoribine or 250 nM CpG ODN for the indicated times. T-bet RNA expression relative to β-actin was determined by Q-RT-PCR.

(F) T-bet RNA expression is elevated in 564Igi B cells. Amounts of T-bet RNA in sorted CD45 (B220)$^+$ splenocytes from the indicated mice were determined, relative to β-actin, by Q-RT-PCR. T-bet expression relative to β-actin was calculated for the 564Igi-*Rag2*$^{-/-}$ samples and expressed relative to T-bet expression (relative to β-actin expression) in C57BL/6. Error bars are standard deviations. The result is representative of three experiments.

loxoribine and anti-IgM (Figure 6D, shaded histograms). Similar results were obtained when the TLR7 agonist R848 was used in place of loxoribine (data not shown).

These results revealed a striking ability of BCR cross-linking to synergize with TLR7 signaling to activate 564Igi B cells.

564Igi$^+$ B Cells Have Elevated *T-bet* Gene Expression In Vivo

The transcription factor T-bet is induced upon B cell activation through TLR9 (Liu et al., 2003) and is responsible for IgG2a class switch recombination (Gerth et al., 2003; Lin et al., 2004; Liu et al., 2003; Peng et al., 2002). Given the predominance of IgG2a Id$^+$ antibodies in 564Igi mice and the possibility that ssRNA is at least partly responsible for the activation of 564Igi B cells in vivo, we wondered whether T-bet expression is induced downstream of TLR7. Figure 6E shows a time course of T-bet RNA induction, measured by quantitative RT-PCR (Q-RT-PCR) after treatment of nontransgenic C57BL/6 B cells with loxoribine. By 48 hr, T-bet was induced to amounts comparable to those induced by CpG.

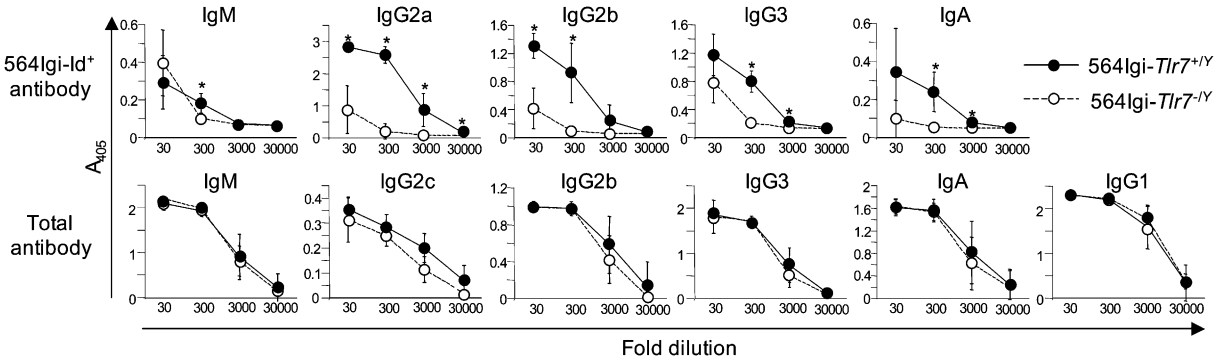

Figure 7. In Vivo Production of 564Igi Id$^+$ Antibody Is Largely TLR7 Dependent

Sera from 564Igi-*Tlr7*$^{-/Y}$ (dotted lines) or 564Igi-*Tlr7*$^{+/Y}$ (solid lines) were tested by ELISA for Id$^+$ antibodies (left) or total antibodies (right) of the indicated isotypes. Shown are average values ± SD for eight (Id$^+$ antibody assay) or seven (total antibody assay) 564Igi-*Tlr7*$^{-/Y}$ mice and nine 564Igi-*Tlr7*$^{+/Y}$ mice. Asterisks denote statistically significant differences ($p < 0.01$) determined by a two-tailed Student's t test. The result is representative of two independent experiments.

If 564Igi B cells were activated in vivo through either TLR7 or TLR9, T-bet mRNA expression should have been elevated in freshly isolated 564 Id$^+$ B cells. We used Q-RT-PCR to compare T-bet RNA expression in splenic B cells isolated from 564Igi-*Rag2*$^{-/-}$ mice to T-bet expression in nontransgenic C57BL/6 splenic B cells. As shown in Figure 6F, T-bet RNA expression was about 5-fold higher in 564Igi$^+$ B cells than in nontransgenic B cells.

These results are consistent with the idea that 564Igi B cells become activated in vivo by TLR7 or TLR9 ligation, which results, among other things, in the induction of *T-bet* gene expression.

Production of 564 Id$^+$ IgG2a Was Largely Dependent on TLR7

The above experiments suggested that 564Igi mice might produce Id$^+$ antibody as a result of B cell activation by an antigen able both to bind to the 564 BCR and to activate either TLR7 or TLR9. To determine whether TLR7 was important in autoantibody production, we bred the 564 heavy and light chain genes onto *Tlr7*$^{-/-}$ mice and measured serum 564 Id$^+$ antibody amounts. Figure 7 (top), shows that, compared to TLR7 wild-type littermate controls, there was a dramatic reduction in serum Id$^+$ IgG2a, IgG2b, IgG3, and IgA but not IgM, in TLR7-deficient 564Igi mice. This reduction was specific to 564 Id$^+$ antibody, as shown by the fact that there was no effect of TLR7 deficiency on total amounts of serum antibodies of the different isotypes (Figure 7, bottom). Amounts of Id$^+$ IgG1 could not be measured because the capture anti-Id is of the IgG1 isotype.

Discussion

Recent studies suggest that dual-specificity ligands that bind both to the BCR and to intracellular TLRs play a crucial role in activation of self reactive B cells. In these studies, B cells expressing an anti-IgG2a rheumatoid factor (RF) proliferated in vitro when treated with immune complexes containing IgG2a and either chromatin (Leadbetter et al., 2002; Viglianti et al., 2003) or RNA (Lau et al., 2005). Activation was dependent on binding of the immune complexes to both the surface anti-IgG2a RF and to TLR9 or TLR7 and required intact TLR signaling. Similarly, transgenic anti-DNA B cells (but not B cells with other specificities) were activated, in vitro, by dsDNA-containing CpG motifs (in this case not part of immune complexes), again in a TLR9-dependent fashion (Viglianti et al., 2003). These experiments suggested a mechanism by which B cells reactive with TLR7 ligands (ssRNA-containing antigens [Diebold et al., 2004; Heil et al., 2004]) or TLR9 ligands (dsDNA-containing antigens [Hemmi et al., 2000]) might initiate systemic autoimmune diseases such as SLE and provided an explanation for why autoantibodies in these diseases often recognize nucleic acid-containing self-antigens.

Consistent with a role for TLRs in autoimmune disease, MyD88, an adaptor protein essential for signaling downstream of multiple TLRs, plays a critical role in autoantibody production in MRL-*lpr/lpr* (Lau et al., 2005) and FcγRIIB-deficient (Ehlers et al., 2006) mice. Similarly, TLR9 is required for class-switched anti-dsDNA production in *lpr/lpr* (Christensen et al., 2005) and FcγRIIB-deficient (Ehlers et al., 2006) mice, although in one study, TLR9 protected MRL-*lpr/lpr* mice from disease (Wu and Peng, 2006). Even healthy individuals produce large numbers of B cells reactive with nuclear and cytoplasmic self-antigens, some of which could presumably act as TLR7 or TLR9 ligands (Wardemann et al., 2003). Here we demonstrate that B cells bearing an RNA-specific BCR (Gavalchin et al., 1987), although functionally and phenotypically anergic by multiple criteria, became activated in vivo to class switch and produce autoantibodies in a largely TLR7-dependent fashion. This highlights a critical vulnerability of the immune system, even in nonautoimmune-prone animals.

Tolerance induction appeared to occur normally in 564Igi mice. There was extensive receptor editing, and those B cells that retained expression of the 564 Id were anergic based on their surface phenotype, exclusion from splenic MZs, and failure to be activated in vitro by BCR crosslinking or LPS treatment. Yet at least a fraction of these B cells were class-switched and secreted IgG autoantibody in vivo. Alternatively, despite the absence of a detectable population of nonanergic Id$^+$ cells in the spleens of 564Igi mice, it is possible that autoantibody-producing cells were never at any time anergic.

The Id^+ antibodies produced on both *Rag2*$^{+/+}$ and *Rag2*$^{-/-}$ backgrounds were predominantly of the IgG2a isotype, which is the predominant isotype of antibodies eluted from the kidneys of diseased SNF1 mice (Gavalchin and Datta, 1987). When 564Igi mice were crossed onto a TLR7-deficient background, there was a dramatic reduction in amounts of Id^+ antibody. Titers of total antibody were unaffected. This implicates TLR7 as critical for the activation of Id^+ 564Igi B cells.

The simplest explanation for the requirement of TLR7 in autoantibody production is that TLR7 was directly activated in 564 Id^+ B cells after delivery of ssRNA to the appropriate compartment by BCR-mediated endocytosis. Consistent with this, 564Igi B cells had elevated amounts of RNA encoding the transcription factor T-bet. T-bet is induced by agonists of TLR7 or TLR9 (Figure 6E; Liu et al., 2003) and plays a direct role in the initiation of IgG2a class switching (Gerth et al., 2003; Lin et al., 2004; Liu et al., 2003; Peng et al., 2002). T-bet is also induced in B cells by the combination of CD40 ligation and IL-12 plus IL-18 (Szabo et al., 2000), but we observed elevated T-bet in B cells from *RAG2*-deficient 564Igi mice that lack T cells. Further support for the direct activation of 564 Id^+ B cells by ssRNA came from our in vitro studies where 564 Id^+ B cells proliferated in response to the TLR7 agonist loxoribine (Akira and Hemmi, 2003; Heil et al., 2003) in combination with suboptimal concentrations of anti-IgM. Loxoribine alone induced relatively little proliferation of Id^+ 564Igi B cells. This suggests that the BCR normally functions not only to deliver ssRNA to TLR7 but also to generate signals that synergize with TLR7-derived signals to induce proliferation. The BCR was also shown to synergize with TLR signals in B cells activated in vitro through TLR9 (Viglianti et al., 2003). TLR7 may also indirectly induce autoantibody production by 564Igi B cells by virtue of its role in pDCs to induce secretion of type I interferon (Vollmer et al., 2005), which would facilitate activation of 564Igi B cells.

The synergy between TLR7 and the BCR in Id^+ 564Igi B cells was surprising given that these cells were anergic. In anergic anti-HEL B cells, synergy between the BCR and TLR9 was completely abolished (Rui et al., 2003). The discrepancy between this result and ours could be due to differences between activation by TLR7 versus TLR9 or could result from differences between signals generated by BCR ligation with anti-IgM (our study) versus signals generated by BCR ligation with a soluble antigen (Rui et al., 2003).

In several other transgenic models, B cells express a BCR reactive with nucleic acid and could potentially be activated by dual ligation of the BCR and TLR7 or TLR9 (reviewed in Fields and Erikson, 2003). Yet in only one of these systems, in mice containing a targeted insertion of the 3H9/56R heavy chain gene, is autoantibody produced on a nonautoimmune-prone background. This heavy chain gene binds dsDNA with high affinity and with an exceptionally large variety of different light chains (Radic et al., 1993). On a BALB/c background, 3H9/56R heavy chain knockin mice produced IgM but no IgG dsDNA antibody (Fukuyama et al., 2005; Li et al., 2002). On a C57BL/6 background, both IgM and IgG dsDNA antibody were produced, but the IgG titers were very low (Fukuyama et al., 2005). These low amounts of IgG anti-DNA were maintained by an FcγRIIB-dependent checkpoint that limited the accumulation of autoreactive plasma cells (Fukuyama et al., 2005). This mechanism was evidently overridden in 564Igi mice, which produced large quantities of IgG 564 Id^+ antibodies.

So why do 564Igi mice produce high titers of IgG autoantibody when similar Ig-transgenic mice do not? It may be in part due to the C57BL/6 genetic background. Although C57BL/6 mice do not spontaneously develop autoimmune disease, they contain genetic loci that contribute to autoimmune disease in some contexts (Bygrave et al., 2004; Bolland et al., 2002). Still, other anti-nucleic acid Ig-transgenic lines maintain tolerance on a C57BL/6 background (Yachimovich et al., 2002). The specificity or avidity of the 564 antibody was likely the determining factor. For example, the physiological self-antigen of 564 may be present at higher levels than the self-antigens recognized by other transgenic BCRs.

Injection of the 564 hybridoma into young, preautoimmune SNF1 mice resulted in the rapid development of kidney disease (Vlahakos et al., 1992). It was not determined whether this pathogenicity required the autoimmune-prone SNF1 background. Here we showed that in 564Igi mice there were Id^+ and $IgG2a^+$ antibodies in the kidneys along with changes visible by EM consistent with mesangioproliferative glomerulonephropathies in human patients. Thus, production of the 564 antibody was sufficient to cause pathology in nonautoimmune-prone C57BL/6 mice.

In summary, the 564Igi system demonstrates that TLR7-dependent processes can result in the activation of autoreactive B cells to class switch and secrete pathogenic antibodies in vivo and lead to renal pathology. This is likely a result of the dual reactivity of autoantigen with the BCR and TLR7.

Experimental Procedures

Mice

All experiments with mice were performed in accordance with the regulations and with the approval of Tufts/NEMC IACUC. C57BL/6 mice were obtained from Jackson Laboratories (Bar Harbor, ME), RAG2-deficient mice on a C57BL/6 background were obtained from Taconic (Hudson, NY), AID-deficient mice on a C57BL/6 background were obtained from Dr. J. Stavnezer (University of Massachusetts Medical School, Worcester, MA) with permission from Dr. T. Honjo (Kyoto University, Kyoto, Japan), and CMV-Cre transgenic mice on a C57BL/6 background were obtained from Dr. J. Chen (Massachusetts Institute of Technology, Cambridge, MA).

The generation of 564Igi heavy chain targeted transgenic mice has been described (Fernandez, 2001). 564Igi light chain targeted transgenic mice were generated by standard methods. A detailed description is provided in Supplemental Data.

564Igi mice on a TLR7-deficient background were obtained by crossing female TLR7 heterozygous mice (Hemmi et al., 2002) with a male homozygous heavy and light chain 564Igi mouse that was also C4 deficient (*C4*$^{-/-}$). All offspring were heterozygous for the heavy and light chain 564Igi insertions and for C4. Experiments were performed with male offspring, which were hemizygous for either the wild-type (+/Y) or knockout (−/Y) of the X-linked *Tlr7* allele.

Flow Cytometry

Cells were stained for flow cytometry according to standard procedures. Propidium iodide (PI) was added just prior to analysis on a FACScalibur flow cytometer (BD Biosciences). B6-256 anti-Id was generated as described in Supplemental Data and coupled to

Alexa 488 and Alexa 647 according to the manufacturer's instructions (Invitrogen Molecular Probes). Other fluorochrome-conjugated antibodies were from BD Biosciences or Southern Biotech and were generally used at 1 μg/ml. For staining cells with ODN 1668, Alexa 488-conjugated ODN 1668 with a phosphorothioate bond at each position (Integrated DNA Technologies) was used at a final concentration of 1 μM.

ELISA

For measurements of 564Igi-Id$^+$ antibodies, ELISA plates were coated with 5 μg/well of purified B6-256 anti-Id hybridoma protein. Bound serum antibody was detected with 1 μg/ml Alkaline Phosphatase (AP)-conjugated isotype-specific goat anti-mouse (Southern Biotech). For measurement of total serum antibodies of different isotypes, wells were coated with 1 μg/ml isotype-specific goat anti-mouse Ig (Southern Biotech) and bound serum antibody detected with AP-conjugated isotype-specific goat anti-mouse Ig (Southern Biotech). AP-conjugated antibody was detected with *p*-nitrophenyl phosphate (pNPP) (Sigma-Aldrich), and ODs were determined in a Spectra Max 340 ELISA plate reader (Molecular Devices).

Immunofluorescence Analysis of Spleen Tissue Sections

Tissue sections were processed as previously described (Oliver et al., 1999). Frozen sections of spleens were stained with MOMA-1 (rat IgG2a, κ; a gift from Dr. Georg Kraal, VU Medical Center, Amsterdam, The Netherlands) developed with goat anti-rat Alexa 647 IgG (Invitrogen), blocked with normal rat serum (PelFreeze), washed, and then stained with a mixture of Alexa 488 mouse anti-564Igi Id (B6-256) and PE-conjugated goat anti-mouse IgM (Southern Biotech). Stained sections were viewed and photographed with a Leica DMRB microscope with a Hamamatsu C4742-95 camera and Openlab software.

Electron, Immunofluorescence, and Light Microscopy Analysis of Kidney Sections

Tissue samples for electron microscopy were first fixed in Trump's fixative for 30 min and then post-fixed in 2% aqueous osmium tetroxide for 20 min at room temperature. The fixed tissue was washed in distilled water twice and en block stained in saturated uranyl acetate in 50% ethanol for 15 min. It was then dehydrated into absolute ethanol, placed in two changes of propylene oxide for 5 min each, and transferred into propylene oxide epoxy resin mixture 1:1 for 2 min and finally into epoxy resin. The cured epoxy blocks were sectioned on an LKB ultra microtome with appropriate glomerular samples thin-sectioned at 30–40 nm and picked up on copper grids. The grids were stained with uranyl acetate and lead citrate. The samples were examined and photographed in a Philips EM 20.

Fresh kidney samples for immunofluorescence studies were frozen in OCT and 4 μm sections cut on a cryostat and mounted on glass slides. The sections were air-dried for 1 hr, dehydrated in PBS, and incubated with primary fluorescein-conjugated antibody solution 1/200 dilution for 1 hr at room temperature. The sections were rinsed in PBS, mounted in Aquamount, and examined and photographed in a Zeiss fluorescence microscope.

Kidneys were removed, fixed in 10% buffered formalin, and embedded in paraffin. 5 μm paraffin sections were stained with periodic acid-Schiff (PAS) and evaluated by light microscopy in a blind manner as previously described (Vlahakos et al., 1992).

Quantitative RT-PCR

Total RNA was prepared with TRIzol reagent (Invitrogen) from splenic B220$^+$ cells sorted on a MoFlo cell sorter (Dako Cytomation). RNA was subsequently repurified with RNeasy columns (Qiagen). cDNA synthesis was performed on 5-fold serial dilutions of RNA with Iscript cDNA synthesis kit (Bio-Rad). Real-time PCR was performed in triplicate for each cDNA reaction with Applied Biosystems TaqMan reaction mix according to the manufacturer's instructions. Further details about the Q-RT-PCR are available in Supplemental Data.

Proliferation Assays

Disaggregated splenocytes were passed through a nylon cell strainer and depleted of red blood cells (RBC) by treatment with Tris-NH_4Cl-BSA at 4°C for 4 min. Cells were washed and resuspended in complete medium (RPMI 1640 plus sodium pyruvate, HEPES, glutamine, 2-mercaptoethanol, nonessential amino acids, and 10% fetal calf serum [FCS]) or DPBS with 5% FCS. To load cells with CFSE, they were washed and resuspended in serum-free RPMI 1640 at 2.5×10^6 cells/ml. CFSE in DMSO was added to a final concentration of 5 μM and cells incubated at room temperature for 5 min. The reaction was stopped by the addition of FCS to 20%. Cells were washed twice and resuspended in complete medium at 1×10^6 cells/ml. Cells were treated with immunostimulatory ODN 1668 (tccatgacgttcctgatgct) or control ODN 1720 (tccatgagcttcct gatgct), both with a phosphorothioate bond at each position and HPLC purified, obtained from Integrated DNA Technologies. Both had less than 0.1 endotoxin units/ml by the kinetic limulus test (Cambrex). LPS stimulations were performed with *E. coli* LPS (Sigma-Aldrich). Loxoribine (InVivogen) was used at a concentration of 250 μM. F(ab′)$_2$ goat anti-mouse IgM μ-chain specific was from Jackson Immunoresearch. After culture, cells were harvested, resuspended in FACS staining buffer, and stained with fluorochrome-conjugated antibodies for FACS analysis as described above.

Calcium Flux Assays

RBC-depleted splenocytes were washed once in DPBS with 5% FCS and resuspended in DPBS with 5% FCS at 5×10^6 cells/ml. Indo-1-AM (Invitrogen) was added to a final concentration of 1 μM from a 1 mM stock in DMSO. Cells were incubated at 37°C for 30 min, washed twice, and resuspended in DPBS with 5% FCS and stained with fluorochrome-conjugated antibodies. 0.5 ml aliquots of cells at 5×10^6/ml were analyzed for Ca^{2+} flux on a MoFlo cell sorter (Dako Cytomation). Cells were stimulated with F(ab′)$_2$ goat anti-mouse IgM, μ chain specific (Jackson Immunoresearch).

Immunofluorescence Staining of HEp-2 Cells

Fixed human HEp-2 cells (Antibodies Inc.) were stained with mouse serum according to the manufacturer's instructions, except that the secondary antibody was either FITC-conjugated F(ab′)$_2$ goat anti-mouse IgG (Jackson Immunoresearch) or FITC-anti-mouse IgG2a (Southern Biotech). Slides were mounted with ProLong Gold antifade reagent (Invitrogen) and digitally photographed with a Nikon E400 fluorescence microscope.

Supplemental Data

Supplemental Data include three figures and Supplemental Results and Experimental Procedures and can be found with this article online at http://www.immunity.com/cgi/content/full/25/3/429/DC1/.

Acknowledgments

We wish to thank A. Poltorak for useful discussions, K. Stephan for performing endotoxin testing and useful discussions, and A. Parmelee for sorting and Ca^{2+} analysis on the MoFlo. We also wish to thank I. Rifkin from Boston University School of Medicine who kindly gave us *Tlr7*$^{+/-}$ females for our breedings. This work was supported by NIH grants AI45104-5 (to T.I.-K.), AI043535 (to H.H.W.), and AI014782-27 (to J.F.K.). T.I.-K. thanks the Eshe Fund for their generous support.

Received: April 28, 2006
Revised: June 26, 2006
Accepted: July 10, 2006
Published online: September 14, 2006

References

Akira, S., and Hemmi, H. (2003). Recognition of pathogen-associated molecular patterns by TLR family. Immunol. Lett. *85*, 85–95.

Barton, G.M., Kagan, J.C., and Medzhitov, R. (2006). Intracellular localization of Toll-like receptor 9 prevents recognition of self DNA but facilitates access to viral DNA. Nat. Immunol. *7*, 49–56.

Bolland, S., Yim, Y.S., Tus, K., Wakeland, E.K., and Ravetch, J.V. (2002). Genetic modifiers of systemic lupus erythematosus in FcgammaRIIB(−/−) mice. J. Exp. Med. *195*, 1167–1174.

Boule, M.W., Broughton, C., Mackay, F., Akira, S., Marshak-Rothstein, A., and Rifkin, I.R. (2004). Toll-like receptor 9-dependent and -independent dendritic cell activation by chromatin-immunoglobulin G complexes. J. Exp. Med. *199*, 1631–1640.

Bygrave, A.E., Rose, K.L., Cortes-Hernandez, J., Warren, J., Rigby, R.J., Cook, H.T., Walport, M.J., Vyse, T.J., and Botto, M. (2004). Spontaneous autoimmunity in 129 and C57BL/6 mice-implications for autoimmunity described in gene-targeted mice. PLoS Biol. *2*, E243. 10.1371/journal.pbio.0020243.

Casellas, R., Shih, T.A., Kleinewietfeld, M., Rakonjac, J., Nemazee, D., Rajewsky, K., and Nussenzweig, M.C. (2001). Contribution of receptor editing to the antibody repertoire. Science *291*, 1541–1544.

Chen, C., Prak, E.L., and Weigert, M. (1997). Editing disease-associated autoantibodies. Immunity *6*, 97–105.

Christensen, S.R., Kashgarian, M., Alexopoulou, L., Flavell, R.A., Akira, S., and Shlomchik, M.J. (2005). Toll-like receptor 9 controls anti-DNA autoantibody production in murine lupus. J. Exp. Med. *202*, 321–331.

Cyster, J.G., Hartley, S.B., and Goodnow, C.C. (1994). Competition for follicular niches excludes self-reactive cells from the recirculating B-cell repertoire. Nature *371*, 389–395.

Diebold, S.S., Kaisho, T., Hemmi, H., Akira, S., and Reis e Sousa, C. (2004). Innate antiviral responses by means of TLR7-mediated recognition of single-stranded RNA. Science *303*, 1529–1531.

Ehlers, M., Fukuyama, H., McGaha, T.L., Aderem, A., and Ravetch, J.V. (2006). TLR9/MyD88 signaling is required for class switching to pathogenic IgG2a and 2b autoantibodies in SLE. J. Exp. Med. *203*, 553–561.

Fernandez, L.P.J. (2001). B cell tolerance to nucleosomes in normal mice and its breakdown in autoimmune-prone mice. PhD thesis, Tufts University, Somerville, Massachusetts.

Fields, M.L., and Erikson, J. (2003). The regulation of lupus-associated autoantibodies: immunoglobulin transgenic models. Curr. Opin. Immunol. *15*, 709–717.

Fukuyama, H., Nimmerjahn, F., and Ravetch, J.V. (2005). The inhibitory Fcgamma receptor modulates autoimmunity by limiting the accumulation of immunoglobulin G+ anti-DNA plasma cells. Nat. Immunol. *6*, 99–106.

Gauld, S.B., Benschop, R.J., Merrell, K.T., and Cambier, J.C. (2005). Maintenance of B cell anergy requires constant antigen receptor occupancy and signaling. Nat. Immunol. *6*, 1160–1167.

Gavalchin, J., and Datta, S.K. (1987). The NZB X SWR model of lupus nephritis. II. Autoantibodies deposited in renal lesions show a distinctive and restricted idiotypic diversity. J. Immunol. *138*, 138–148.

Gavalchin, J., Seder, R.A., and Datta, S.K. (1987). The NZB X SWR model of lupus nephritis. I. Cross-reactive idiotypes of monoclonal anti-DNA antibodies in relation to antigenic specificity, charge, and allotype. Identification of interconnected idiotype families inherited from the normal SWR and the autoimmune NZB parents. J. Immunol. *138*, 128–137.

Gerth, A.J., Lin, L., and Peng, S.L. (2003). T-bet regulates T-independent IgG2a class switching. Int. Immunol. *15*, 937–944.

Goodnow, C.C., Sprent, J., Fazekas de St Groth, B., and Vinuesa, C.G. (2005). Cellular and genetic mechanisms of self tolerance and autoimmunity. Nature *435*, 590–597.

Healy, J.I., Dolmetsch, R.E., Timmerman, L.A., Cyster, J.G., Thomas, M.L., Crabtree, G.R., Lewis, R.S., and Goodnow, C.C. (1997). Different nuclear signals are activated by the B cell receptor during positive versus negative signaling. Immunity *6*, 419–428.

Heil, F., Ahmad-Nejad, P., Hemmi, H., Hochrein, H., Ampenberger, F., Gellert, T., Dietrich, H., Lipford, G., Takeda, K., Akira, S., et al. (2003). The Toll-like receptor 7 (TLR7)-specific stimulus loxoribine uncovers a strong relationship within the TLR7, 8 and 9 subfamily. Eur. J. Immunol. *33*, 2987–2997.

Heil, F., Hemmi, H., Hochrein, H., Ampenberger, F., Kirschning, C., Akira, S., Lipford, G., Wagner, H., and Bauer, S. (2004). Species-specific recognition of single-stranded RNA via toll-like receptor 7 and 8. Science *303*, 1526–1529.

Hemmi, H., Takeuchi, O., Kawai, T., Kaisho, T., Sato, S., Sanjo, H., Matsumoto, M., Hoshino, K., Wagner, H., Takeda, K., and Akira, S. (2000). A Toll-like receptor recognizes bacterial DNA. Nature *408*, 740–745.

Hemmi, H., Kaisho, T., Takeuchi, O., Sato, S., Sanjo, H., Hoshino, K., Horiuchi, T., Tomizawa, H., Takeda, K., and Akira, S. (2002). Small anti-viral compounds activate immune cells via the TLR7 MyD88-dependent signaling pathway. Nat. Immunol. *3*, 196–200.

Hippen, K.L., Tze, L.E., and Behrens, T.W. (2000). CD5 maintains tolerance in anergic B cells. J. Exp. Med. *191*, 883–890.

Lau, C.M., Broughton, C., Tabor, A.S., Akira, S., Flavell, R.A., Mamula, M.J., Christensen, S.R., Shlomchik, M.J., Viglianti, G.A., Rifkin, I.R., and Marshak-Rothstein, A. (2005). RNA-associated autoantigens activate B cells by combined B cell antigen receptor/Toll-like receptor 7 engagement. J. Exp. Med. *202*, 1171–1177.

Leadbetter, E.A., Rifkin, I.R., Hohlbaum, A.M., Beaudette, B.C., Shlomchik, M.J., and Marshak-Rothstein, A. (2002). Chromatin-IgG complexes activate B cells by dual engagement of IgM and Toll-like receptors. Nature *416*, 603–607.

Li, Y., Li, H., Ni, D., and Weigert, M. (2002). Anti-DNA B cells in MRL/lpr mice show altered differentiation and editing pattern. J. Exp. Med. *196*, 1543–1552.

Lin, L., Gerth, A.J., and Peng, S.L. (2004). CpG DNA redirects class-switching towards "Th1-like" Ig isotype production via TLR9 and MyD88. Eur. J. Immunol. *34*, 1483–1487.

Liu, N., Ohnishi, N., Ni, L., Akira, S., and Bacon, K.B. (2003). CpG directly induces T-bet expression and inhibits IgG1 and IgE switching in B cells. Nat. Immunol. *4*, 687–693.

Liu, S., Velez, M.G., Humann, J., Rowland, S., Conrad, F.J., Halverson, R., Torres, R.M., and Pelanda, R. (2005). Receptor editing can lead to allelic inclusion and development of B cells that retain antibodies reacting with high avidity autoantigens. J. Immunol. *175*, 5067–5076.

Mohan, C., Adams, S., Stanik, V., and Datta, S.K. (1993). Nucleosome: a major immunogen for pathogenic autoantibody-inducing T cells of lupus. J. Exp. Med. *177*, 1367–1381.

Murakami, M., Tsubata, T., Okamoto, M., Shimizu, A., Kumagai, S., Imura, H., and Honjo, T. (1992). Antigen-induced apoptotic death of Ly-1 B cells responsible for autoimmune disease in transgenic mice. Nature *357*, 77–80.

Oliver, A.M., Martin, F., and Kearney, J.F. (1999). IgMhighCD21high lymphocytes enriched in the splenic marginal zone generate effector cells more rapidly than the bulk of follicular B cells. J. Immunol. *162*, 7198–7207.

Peng, S.L., Szabo, S.J., and Glimcher, L.H. (2002). T-bet regulates IgG class switching and pathogenic autoantibody production. Proc. Natl. Acad. Sci. USA *99*, 5545–5550.

Phan, T.G., Amesbury, M., Gardam, S., Crosbie, J., Hasbold, J., Hodgkin, P.D., Basten, A., and Brink, R. (2003). B cell receptor-independent stimuli trigger immunoglobulin (Ig) class switch recombination and production of IgG autoantibodies by anergic self-reactive B cells. J. Exp. Med. *197*, 845–860.

Qian, Y., Santiago, C., Borrero, M., Tedder, T.F., and Clarke, S.H. (2001). Lupus-specific antiribonucleoprotein B cell tolerance in non-autoimmune mice is maintained by differentiation to B-1 and governed by B cell receptor signaling thresholds. J. Immunol. *166*, 2412–2419.

Radic, M.Z., Mackle, J., Erikson, J., Mol, C., Anderson, W.F., and Weigert, M. (1993). Residues that mediate DNA binding of autoimmune antibodies. J. Immunol. *150*, 4966–4977.

Rui, L., Vinuesa, C.G., Blasioli, J., and Goodnow, C.C. (2003). Resistance to CpG DNA-induced autoimmunity through tolerogenic B cell antigen receptor ERK signaling. Nat. Immunol. *4*, 594–600.

Szabo, S.J., Kim, S.T., Costa, G.L., Zhang, X., Fathman, C.G., and Glimcher, L.H. (2000). A novel transcription factor, T-bet, directs Th1 lineage commitment. Cell *100*, 655–669.

Takeda, K., Kaisho, T., and Akira, S. (2003). Toll-like receptors. Annu. Rev. Immunol. *21*, 335–376.

Viglianti, G.A., Lau, C.M., Hanley, T.M., Miko, B.A., Shlomchik, M.J., and Marshak-Rothstein, A. (2003). Activation of autoreactive B cells by CpG dsDNA. Immunity *19*, 837–847.

Vlahakos, D.V., Foster, M.H., Adams, S., Katz, M., Ucci, A.A., Barrett, K.J., Datta, S.K., and Madaio, M.P. (1992). Anti-DNA antibodies form immune deposits at distinct glomerular and vascular sites. Kidney Int. *41*, 1690–1700.

Vollmer, J., Tluk, S., Schmitz, C., Hamm, S., Jurk, M., Forsbach, A., Akira, S., Kelly, K.M., Reeves, W.H., Bauer, S., and Krieg, A.M. (2005). Immune stimulation mediated by autoantigen binding sites within small nuclear RNAs involves Toll-like receptors 7 and 8. J. Exp. Med. *202*, 1575–1585.

Wakeland, E., Morel, L., Achey, K., Yui, M., and Longmate, J. (1997). Speed congenics: a classic technique in the fast lane (relatively speaking). Immunol. Today *18*, 472–477.

Wardemann, H., Yurasov, S., Schaefer, A., Young, J.W., Meffre, E., and Nussenzweig, M.C. (2003). Predominant autoantibody production by early human B cell precursors. Science *301*, 1374–1377.

Wu, X., and Peng, S.L. (2006). Toll-like receptor 9 signaling protects against murine lupus. Arthritis Rheum. *54*, 336–342.

Xu, H., Li, H., Suri-Payer, E., Hardy, R.R., and Weigert, M. (1998). Regulation of anti-DNA B cells in recombination-activating gene-deficient mice. J. Exp. Med. *188*, 1247–1254.

Yachimovich, N., Mostoslavsky, G., Yarkoni, Y., Verbovetski, I., and Eilat, D. (2002). The efficiency of B cell receptor (BCR) editing is dependent on BCR light chain rearrangement status. Eur. J. Immunol. *32*, 1164–1174.